

# **Copper coarse particle flotation: frother and collector optimization as a function of interfacial phenomena**

Faustino, L.M.<sup>1</sup>; Silva, W.C.<sup>1</sup>, Martins, A.R.<sup>1</sup>, Saavedra C.<sup>1</sup>

<sup>1</sup> Clariant International Ltd

## **Abstract**

Floating particles at a coarse size offers significant technical, economic, and sustainability benefits, as the most profitable tailings management strategy. Coarse Particle Flotation (CPF) is determinant for Tailings Scavenging (TS) circuits and Coarse Gangue Rejection (CGR). However, at the same time turbulence is imperative for bubble particle collision, a high mechanical energy dissipation rate that increases the centrifugal force leads to the detachment of coarse particles, unless a high enough contact angle and bubble attachment is established. In this context, this paper discusses the causes and effect of specialty chemicals regarding the floatability of coarse and unliberated chalcopyrite particles. The new collector and frother for copper CPF were compared to standard collectors by the light of contact angle with chalcopyrite and quartz, surface tension, bubble size distribution, froth stability and rheological aspects and interpreted to the recovery of copper from a Cu-Mo coarse particle flotation. Fundamental studies with chalcopyrite showed that the optimized frother for CPF provided a specific bubble size distribution that favored the increase in the collection efficiency of coarse particles due to enhanced microrheological properties that hinders coarse particle settling and enables higher stability of bubble-coarse particle aggregates. Furthermore, the new developed collectors increased the contact angle of unliberated chalcopyrite, resulting in efficient attachment and stability, yielding a recovery improvement from 78.7% to 80.9% with 10 percentage point increase in copper recovery in the +210  $\mu\text{m}$  size fraction and 10 percentage point increase in the +150  $\mu\text{m}$ .

**Keywords:** Coarse Particle Flotation, Collectors, Frothers, Bubble-Particle Stability, Hydrodynamics

## 1. Introduction

The recovery of coarse particles in conventional flotation cells remains a persistent challenge in mineral processing, as particles larger than 100  $\mu\text{m}$  have low collision efficiency with bubbles and are prone to detachment depending on the gravitational and hydrodynamic forces balance (ANZOOM; BOURNIVAL; ATA, 2024). Considering the Coarse-particle flotation (CPF) cells, the typical effective flotation upper limit is 150–200  $\mu\text{m}$ . This technology combines density and wettability differentiating properties, once it operates with an injection of water plus chemical reagents from the bottom of the cell to fluidize a bed of particles coming from the pulp fed in the top. Gas is introduced separately, with bubbles rising through the fluidized bed (ANZOOM; BOURNIVAL; ATA, 2024; KOHLMUENCH et al., 2018; REGINO et al., 2020).

Therefore, besides bubble-particle collision and adhesion, the rheology of the three-phase suspension — i.e., its flow resistance, effective viscosity, and microstructure — controls whether particle–bubble aggregates will be successfully collected in the thin froth layer. CPF new technologies minimize local turbulence and provide upward fluid velocities proper to support coarse aggregates, by using froth-feeding to transport coarse and dense attached particles. In CPF systems like the HydroFloat<sup>®</sup>, the pulp behaves more like a dense medium, multiphase suspension than a dilute slurry. Its rheology — i.e., the effective viscosity, yield stress, and energy dissipation pattern — determines whether coarse particle–bubble aggregates survive or detach. The fluidized bed must be fluid enough to enable selective transport but structured enough to hinder microturbulence to preclude bubble-coarse particle detachment (ISLAM; NGUYEN, 2019; LI; YUAN, 2022; OPOKU et al., 2025).

The two main failure modes of bubble-coarse particle aggregates flotation are: (i) liquid film rupture and collapse due to particle weight and (ii) drop-back, that is the fall back of the aggregates into the pulp because the froth cannot support their mass. Therefore, the higher the hydrophobicity, the higher the chances of sustainable attachment of coarse particles onto coarse/mid-size bubbles. On the contrary, the lower the viscosity of the system, the higher the chances of sedimentation or drop-back (XING et al., 2024; WANG et al., 2020; ZHENG et al., 2012).

In this context, chemical reagents are key to overcoming these limitations, once the fine tuning of the interfacial phenomena can only be done by using specific collectors,

frothers and modifiers. Specialty collectors for CPF increase particle hydrophobicity, enhancing attachment probability and promoting stronger bubble–particle aggregates, while the specific frothers control bubble size, surface elasticity, and froth rheology, improving aggregate stability even under turbulent conditions. Thus, the synergistic action of these reagents addresses both kinetic and thermodynamic constraints of coarse particle flotation, enabling the recovery of fractions that would otherwise be lost (KHOSHDAST, 2011; FEO; LASTRA, 2019; PAWLISZAK, 2024; ANZOOM; BOURNIVAL; ATA, 2024).

In this context, this paper discusses the effect of specialty chemicals regarding the floatability of coarse and unliberated chalcopyrite particles. The performance of a specialty collector and frother was compared with standard thiol collectors by the light of copper recovery, conveying the influence of the new chemistry in the contact angle with chalcopyrite and quartz, surface tension, bubble size distribution, froth stability plus rheological aspects.

## **2. Methodology**

### **2.1 Samples and characterization**

A copper–molybdenum sulphide ore sample from northern Chile was selected for bench-scale flotation tests and rheological characterization. The sample was already fully sized below ASTM mesh 10 (2.0 mm). Elemental composition (Cu, Fe, and Mo) was determined by X-ray fluorescence (XRF). Particle size distribution was obtained via wet sieving using ASTM standard sieves (meshes 70, 100, 150, 200, 270, 400, and –400). Quantitative mineralogical analysis was performed using QEMSCAN to identify mineral species, their associations in the flotation feed, and the liberation of valuable minerals by particle size fraction.

### **2.2 Flotation reagents**

Five different collectors were tested in the bench scale flotation cell: 1- Clariant's collector for CPF HOSTAFLOT 20517; 2- Standard collector (the incumbent collector

used for CPF in the plant); 3- Sodium isopropyl xanthate (SIPX); 4- Sodium isobutyl xanthate (SIBX); 5- Potassium amyl xanthate (PAX).

The collectors were evaluated using FLOTANOL M as the standard frother, selected for its relatively weak performance in coarse particle flotation, to specifically assess the strength of the tested collectors. Flotation tests were conducted at fixed dosages of 5 g/t for the collectors, 12 g/t for the frother, and 15 g/t of diesel as a molybdenite collector. A low collector dosage was intentionally applied to enhance sensitivity to performance differences. The pH of all tests was maintained at 8.5 using lime (CaO).

### **2.3 Bench scale flotation tests**

For the bench scale batch flotation tests, 1,250 g sub-samples were ground in a Marcy steel ball mill (5.4 L capacity) at 67 % solids, achieving a  $P_{80}$  of 238  $\mu\text{m}$ . The ground material was diluted with tap water to adjust the solids content to 38 % in the flotation cell. Tests were performed using an Agitair LA-500 flotation machine equipped with a 2.5 L cell, operating at 1,200 rpm with an airflow rate of 10 L/min. Samples were conditioned for 2 minutes, followed by 12 minutes of flotation. The pH was maintained at 8.5 using lime (CaO).

Copper recovery and copper recovery by particle size were the primary response variables. The following size fractions were analysed: +210  $\mu\text{m}$ , -210+150  $\mu\text{m}$ , -150+105  $\mu\text{m}$ , -105+75  $\mu\text{m}$ , -53+37  $\mu\text{m}$ , and -37  $\mu\text{m}$ . These fractions encompassed a wide particle size range, with particular emphasis on coarse particles, as improvements in these size classes can substantially enhance overall flotation efficiency.

### **2.4 Contact angle**

The contact angle of the natural and collector coated minerals was determined by the Washburn capillary rise method. The Washburn method uses the developed mathematical correlation of the rate at which the liquid is drawn through the bed of particles with the contact angle (WASHBURN, 1921). This method requires a careful preparation of two homogeneous beds with identical and reproducible packing of particles. With this

purpose, 16 grams of purified minerals (chalcopyrite and quartz) were previously conditioned for 30 minutes with 200 mL of reagents solutions under determined concentrations at pH 8.5 and  $21 \pm 1$  °C; The sample was filtered and washed with distilled water to remove the excess of reagent; The sample was dried under vacuum and 40°C until dry mass stability was reached. Thereafter, a known weight of the dry mineral powder ( $3.0000 \pm 0.0001$  g) was sampled and loaded into a capillary glass tube, in which a porous paper closes its end (for solids containment) and allows fluid percolation. N-hexane was used as the perfectly wetting liquid while distilled water (pH 8.5 and  $21 \pm 1$  °C) were used as the test liquids.

The equipment software computed the material constant of the bed structure (permeability constant), which is an essential parameter in the calculation of the contact angle according to the Washburn equation. The wetting process is thereafter performed using the other identical sample, this time, with the test liquid, for which the contact angle is being measured. The rate of penetration is again computed by measuring the mass of liquid adsorbed per unit time. The contact angle,  $\Theta$ , is then calculated using the Washburn equation.

## **2.5 Surface tension and bubble size**

Surface tension and bubble size were measured in order to characterize the frothers FLOTANOL M and FLOTANOL C07. The equipment used to determine the surface tension in function of the varying concentration of surfactant was the Krüss Tensiometer (K100), adopting the Wilhelmy plate method to measure the surface tension of the solutions in constant temperature ( $21 \pm 1$  °C).

The determination of bubble size was held in an experimental apparatus, coupling the Anglo Platinum Bubble Sizer device (ABPS-Stone Three) to the bench scale flotation cell (Agitair LA-500), that was filled with the tap water or prepared reagent solutions (frother and/or collector) at  $21 \pm 1$  °C and pH = 8.5. For all measurements rotation of  $1200 \text{ min}^{-1}$  with airflow rate at 10 L/min were fixed parameters. The ABPS captures photos of rising bubbles in the probe as described by Venkatesan et al. (2014) and a software analyzes the bubble images.  $D_{3,2}$  were obtained for a number of concentrations and these variables were then plotted in function of the surfactant concentration (mg/L).

## 2.6 Fluidized bed rheology

The coarse particle ore, same slurry as the flotation feed, was conditioned with the required collectors and frothers (dosages specified in each test series) prior to aeration to simulate the fluidized bed with bubbles. Froths were generated directly within the rheometer measurement cup (in-situ method). All experiments were performed at room temperature ( $21 \pm 1$  °C).

Rheological measurements were conducted using a Thermo Scientific HAAKE Viscotester (Thermo Fisher Scientific, Germany) operating in controlled-rate (CR) mode, equipped with a vane-in-cup geometry to reduce wall slip and preserve the sample structure. The vane tool (FL22 4B/SS) had a diameter of 22 mm and a height of 16 mm, positioned concentrically in a cylindrical cup with an internal radius  $\geq 32$  mm to avoid wall effects. Torque and angular displacement were continuously recorded using the instrument's standard data acquisition settings.

For the in-situ method, 50 mL of conditioned slurry was placed in the rheometer cup, and froth was generated by briefly rotating the vane at  $40 \text{ rad}\cdot\text{s}^{-1}$  while simultaneously introducing compressed air, at a flow rate of  $1 \text{ L}\cdot\text{min}^{-1}$  through a capillary tube. Rheological measurements commenced within 180 s of froth formation.

Each measurement sequence comprised the following steps: 1- Pre-shear: The froth was subjected to a high shear rate of  $40 \text{ s}^{-1}$  for 90 s to standardize shear history, and maintain the solids in suspension. 2- Steady shear flow curve: Shear rate was logarithmically ramped down from  $100 \text{ s}^{-1}$  to  $0.01 \text{ s}^{-1}$ .

Apparent viscosity and shear stress were recorded, and rheological parameters were extracted using the HAAKE RheoWin software. Flow curve data were fitted to the Herschel–Bulkley model to obtain yield stress ( $\tau_0$ ), consistency index (K), and flow index (n) for the evaluated frothers. Apparent viscosity values were determined as a function of shear rate.

### **3. Results and Discussion**

#### **3.1 Coarse Particle Flotation case study**

Coarse-particle flotation (CPF) technology was designed to recover value-bearing particles at much larger sizes ( $> 210\ \mu\text{m}$ ) than conventional cells/columns. The fact of this flotation study being conducted in a conventional mechanical cell was the challenge proposed by Clariant chemicals to yield higher recovery in the  $+210\ \mu\text{m}$ .

##### **3.1.1 Characterization of the CPF feed**

The conventional cell flotation feed was characterized by wet sieving and QEMSCAN to evaluate which fraction of the ore would be recoverable. Figure 1a conveys the particle size distribution of the Coarse Particle Flotation Feed (CPFF), that was used in the flotation and rheology analysis. The PSD reveals that 50% of the particles (P50) are smaller than  $92\ \mu\text{m}$  and P80 is  $238\ \mu\text{m}$ . Moreover, 1b shows that 36% of the particles are bigger than  $210\ \mu\text{m}$ .

Figure 2 conveys through the copper distribution analysis, that 42.2% of copper is found in the  $+210\ \mu\text{m}$  and 55.1% is above  $150\ \mu\text{m}$ . A significant challenge to yield high Copper recovery in a conventional mechanical cell, to a greater extent considering the unliberated chalcopyrite particles in this coarser fraction.

Figure 3a presents the QEMSCAN analysis, showing a composition of 5.4% of sulfide minerals and the presence of quartz (25%) complex silicates such as feldspars and chlorite (56%). Figure 3b shows that the sulfide minerals are mainly pyrite, a gangue mineral (59% of the sulfides) and the mineral of interest, chalcopyrite.

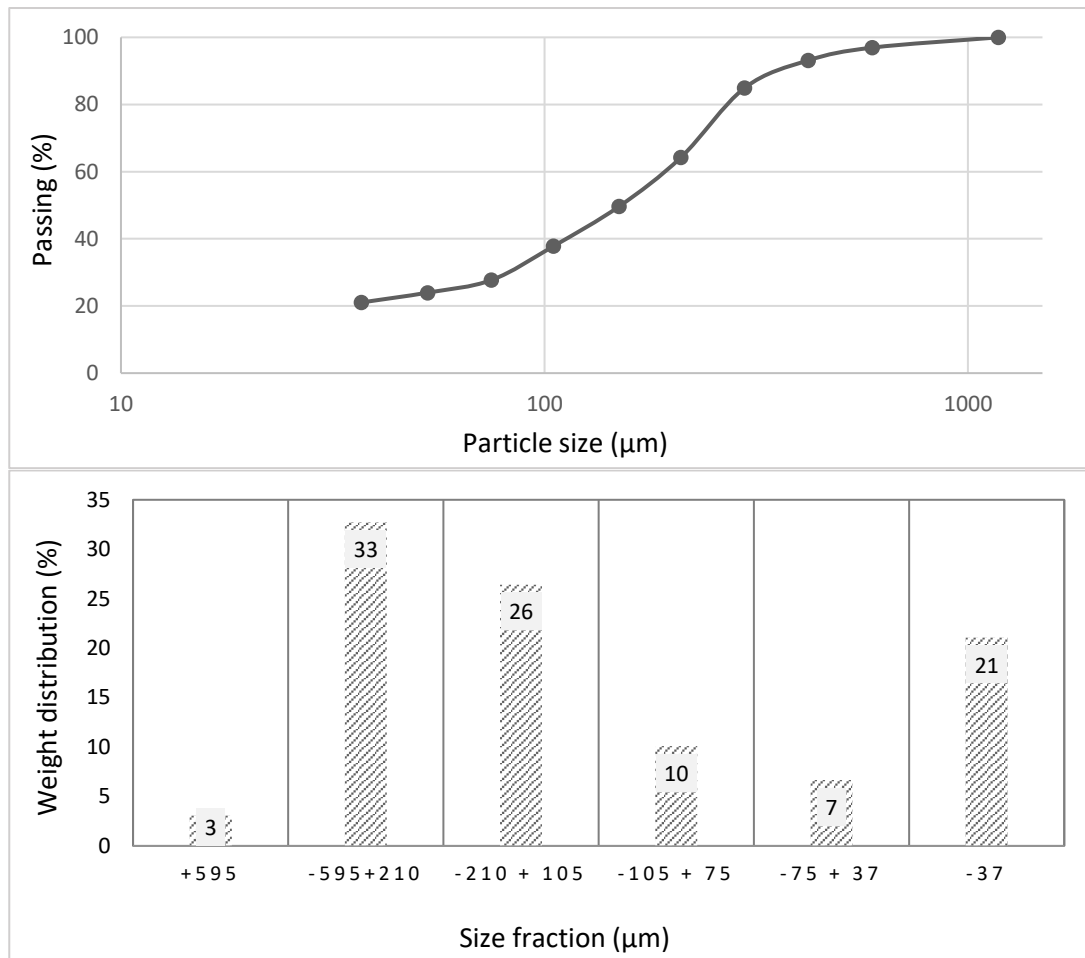


Figure 1. Flotation feed size analysis by wet sieving: Particle size distribution (a) and weight distribution by size fraction (b)

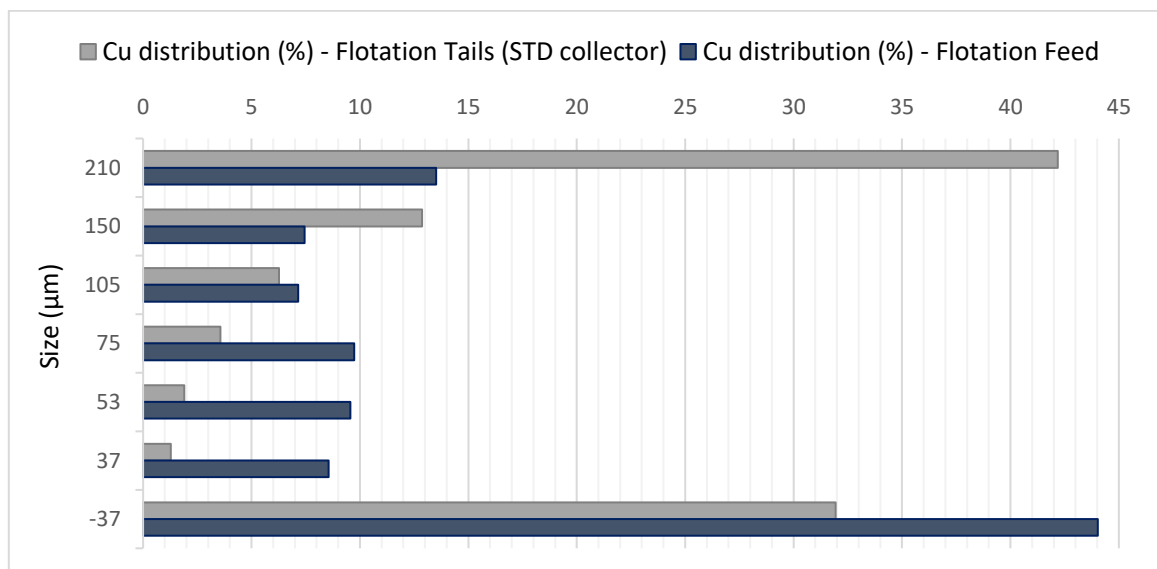


Figure 2. Copper distribution in the Coarse Particle Flotation Feed (CPFF)



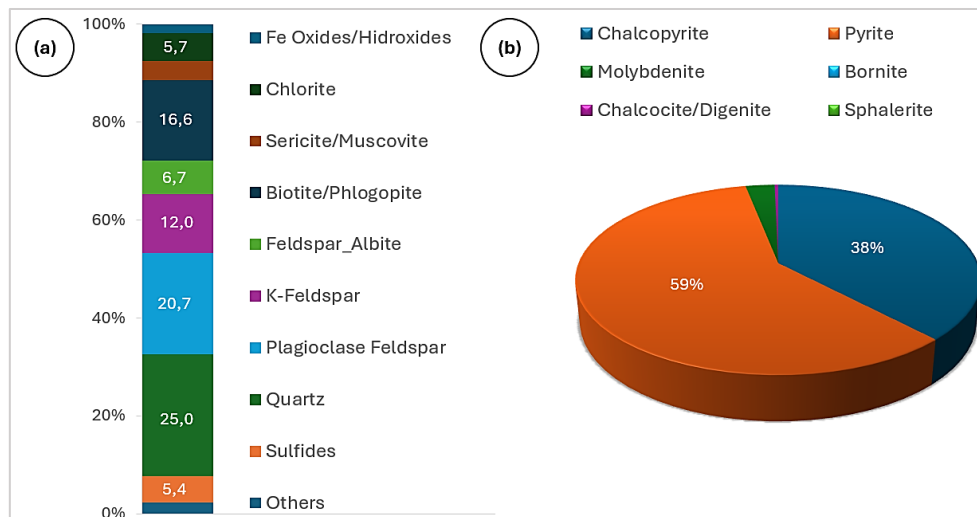


Figure 3. Flotation feed mineralogy by QEMSCAN: Modal mineralogy (a) and sulfide bearing minerals (b)

Figure 4 highlights the mineralogical associations found in the CPFF. Only 63% of chalcopryrite is liberated, whereas the remainders are associated with quartz and complex silicates, as seen in Figure 3C. The main locked chalcopryrite grains are found in the +106  $\mu\text{m}$  fraction and most middlings are shown in the +150  $\mu\text{m}$ . Therefore, the challenge posed by this sample is in the recovery of the +150  $\mu\text{m}$ , considering the major part of the Copper is concentrated in this fraction (Figure 2).

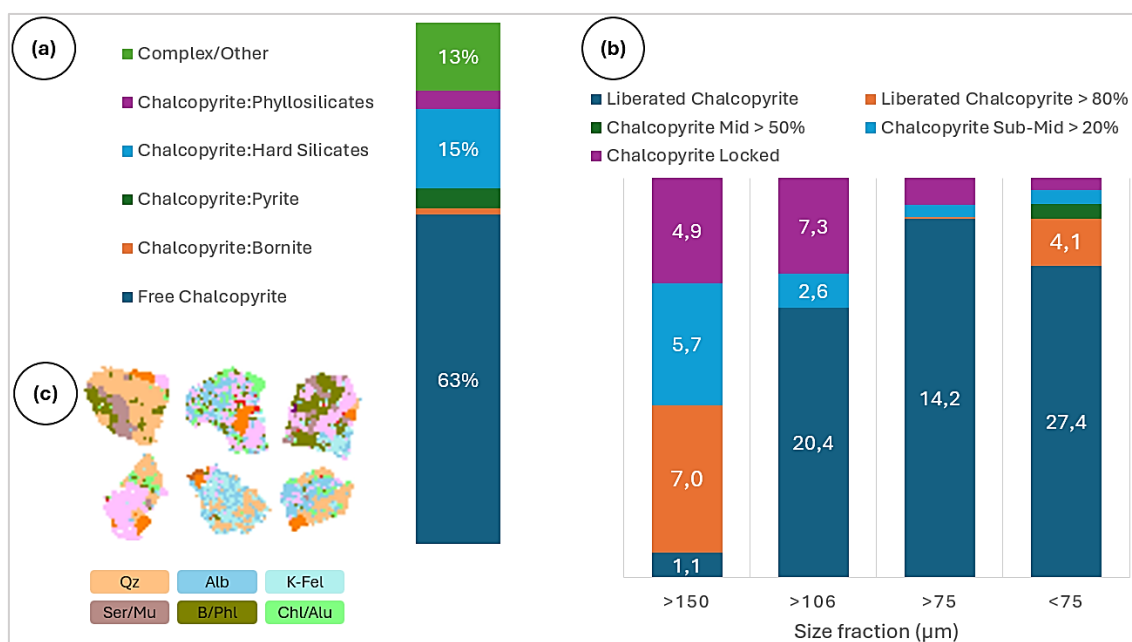


Figure 4. Liberation analysis of the flotation feed by QEMSCAN: Mineral associations with chalcopryrite (a), liberation analysis by size fraction (b) and mapping of main mineral associations with chalcopryrite.

Unliberated chalcopyrite particles should be floated as a result of specific collectors adsorption onto exposed chalcopyrite surfaces as small as 20% of the specific surface area, creating hydrophobic patches that are sufficient for bubble attachment. Therefore, a tailor-made collector was developed for low liberation chalcopyrite coarse particles. The collector coated chalcopyrite was studied to verify the new chemistry would result in higher contact angles, enhanced bubble size distribution and consequently higher copper recovery in the +210  $\mu\text{m}$  fraction. With this purpose, the evaluated parameters for the collector optimization were Redox potential, contact angle and the resultant bubble size distribution as a function of the synergism between collectors and the frother FLOTANOL M.

### 3.1.2 Redox potential: Lower oxidation effect to improve collector adsorption

Oxide or sulfate ( $\text{SO}_4^{2-}$ ) surface films decrease the mineral's hydrophobicity. Therefore, the reduction or chemical removal of these oxidized species—through sulfidization or reducing pretreatments —facilitates collector chemisorption onto the underlying sulfide ( $\text{S}^{2-}$ ) surface, thereby enhancing the contact angle of chalcopyrite (MIKI et al., 2017). In this context, Figure 5 shows that the standard collector significantly increases the ORP after its dosage, up to 200 mV, whereas the HOSTAFLOT 20517 and the xanthate collectors keep the ORP between 50 and 100 mV.

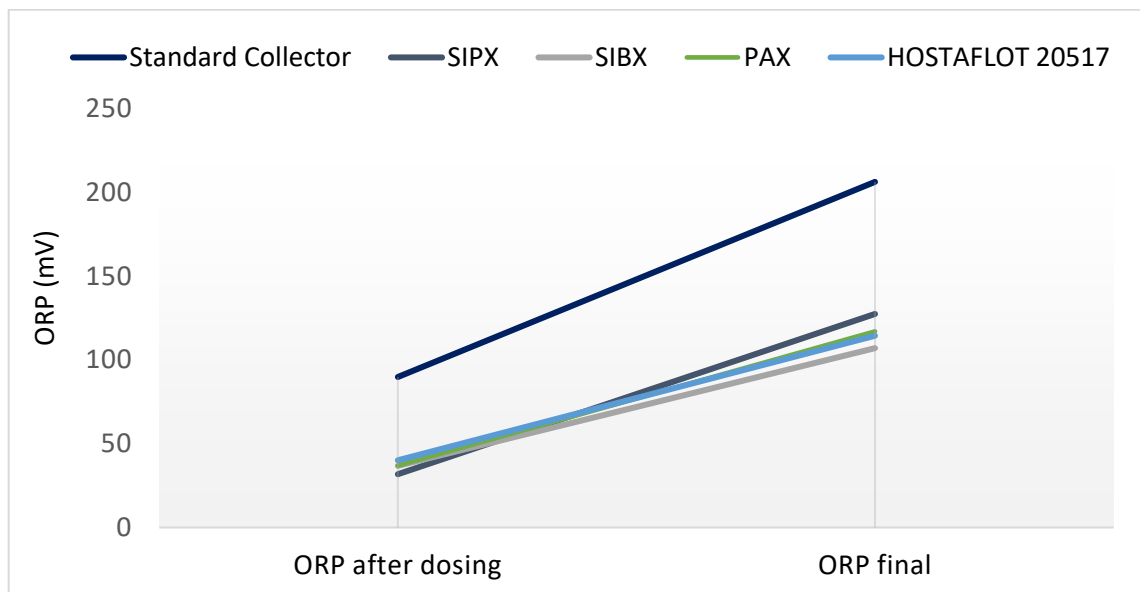


Figure 5. ORP values right after dosing the collector and by the end of the flotation trials at pH 8.5

This means that the standard collector might have oxidized the chalcopyrite surface or that this chemistry is an oxidized collector. Xanthates ( $\text{ROCS}_2^-$ ) often oxidize to dixanthogen  $(\text{ROCS}_2)_2$  during collector adsorption or redox reactions. Shorter-chain xanthates (like SIPX) are more easily oxidized, consuming more electrons and lowering the system's redox potential (ORP). Diversely, longer-chain xanthates, such as PAX, are more stable and resistant to oxidation, which results in a more oxidizing media, with a higher ORP, during and after conditioning. Therefore, the longer the carbon chain, the less reducing the xanthate is, so PAX maintains a higher ORP.

Although a longer chain collector should contribute to increase the contact angle (surface hydrophobicity), a collector that keeps higher ORP is weaker in terms of adsorption, translated by lower surface coverage or physisorption, that can result in lower contact angle and lower selectivity for chalcopyrite flotation (YELLOJI; NATARAJAN, 1989; CASTELLÓN et al., 2022; YANG et al., 2022). Conversely, the HOSTAFLOT 20517 is a stronger collector compared to SIBX and SIPX and keeping a smaller ORP in the flotation pulp, proving a stronger metal-collector interaction. This discussion will be supported by the higher recovery of coarse chalcopyrite particles and contact angle results, discussed in the following sections.

### **3.1.3 Contact angle: Increased contact angle to enhance bubble-particle stability**

Flotation requires a minimum (critical) contact angle for a particle of given size to form a stable bubble-particle aggregate; that critical angle increases with particle size and depends on bubble size, hydrodynamics and cell type. Coarse particles therefore need substantially higher contact angles than fines. For instance, unliberated chalcopyrite  $> \sim 210 \mu\text{m}$  require an advancing contact angle in the range  $\approx 80^\circ$  for an efficient attachment and stability of the coarse and dense particles by the bubbles (ANZOOM; BOURNIVAL; ATA, 2023).

Figure 6a proves the discussed over Figure 5, showing an increase on the contact angle of chalcopyrite from  $59^\circ$  to  $64^\circ$  with the standard collector at 1 g/t, whereas with the new collector HOSTAFLOT 20517 the obtained contact angle values achieved  $80^\circ$  at 5 g/t. Besides showing stronger hydrophobization potential, the H. 20517 was more selective against quartz, showing a maximum contact angle of  $24^\circ$ , not sufficient to fines and intermediate particles of the gangue minerals (CRAWFORD; RALSTON, 1988).

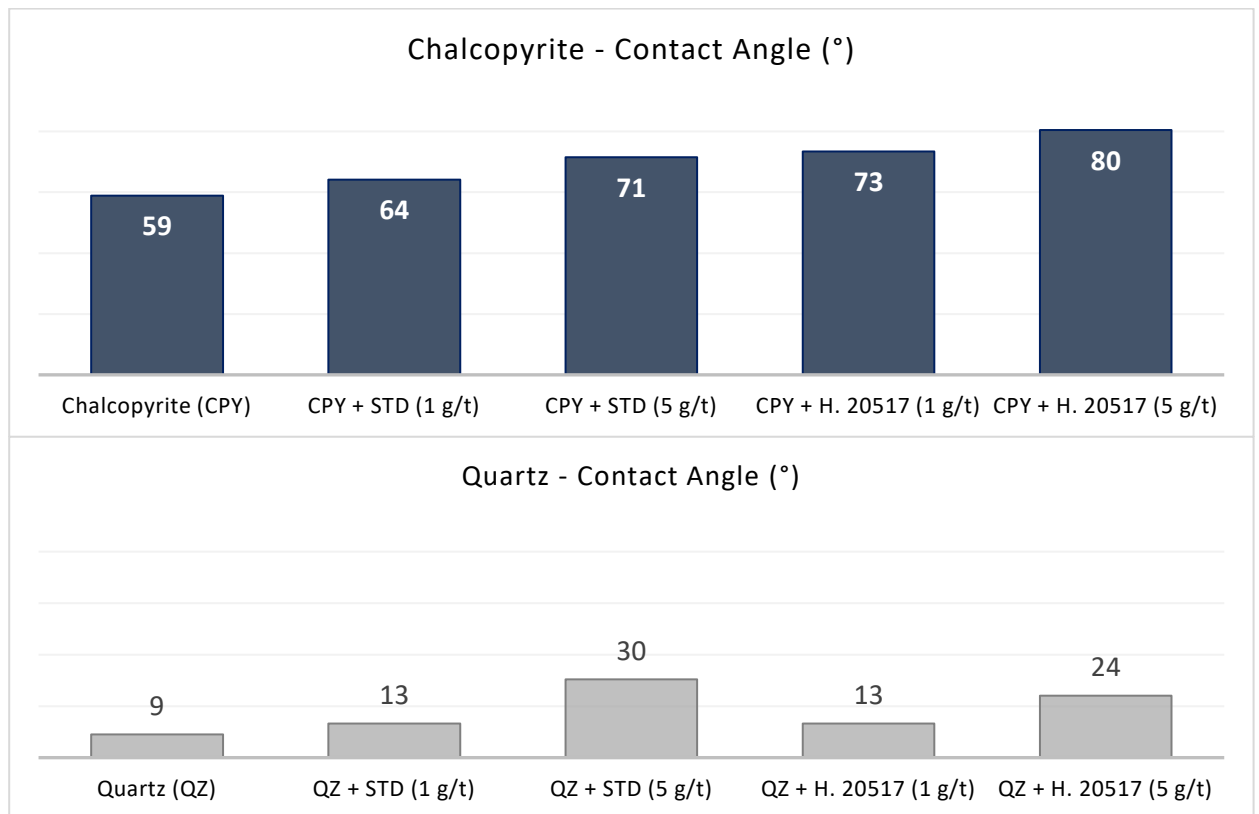


Figure 6. Contact angle of chalcopyrite (a) and quartz (b) with the standard collector and with HOSTAFLOT 20517 at different dosages and pH = 8.5

Therefore, the collector HOSTAFLOT 20517 increases the probability of the bubbles with coarse and top size particles. Additionally, considering this coarse fraction has poor liberation (< 50%), a stronger collector is imperative for successful recovery.

### 3.1.4 The synergistic effect of collector and frother to optimize bubble size distribution

Collectors, through adsorption on sulphide mineral surfaces, enhance the probability of attachment by lowering the solid–liquid interfacial energy. Additionally, collectors adsorbed onto the mineral surface contributes for faster thin-film rupture between bubbles and hydrophobic particles, promoting stable bubble–particle aggregates and higher kinetics (CASTELLÓN et al., 2022).

As seen in Figure 7, the synergy of the collector H. 20517 and FLOTANOL M. reduces bubble size variability, leading to a narrower BSD that enhances selectivity and

recovery. This feature was only identified in the performance of the specialty collector for CPF. Conversely, the standard collector combined with the frother FLOTANOL M significantly decreased its performance in generating smaller bubbles, instead the negative synergism between the chemicals resulted in a broad BSD with 22% of the bubbles  $> 3.0$  mm.

This finding highlights the importance of optimizing the collector–frother chemistry and dosage to maximize the recovery of coarse chalcopyrite in CPF cells, once one can interfere in another’s performance. For the FLOTANOL M, an alcohol based frother, the collector HOSTAFLOT 20517 presented superior results, as discussed in the following section.

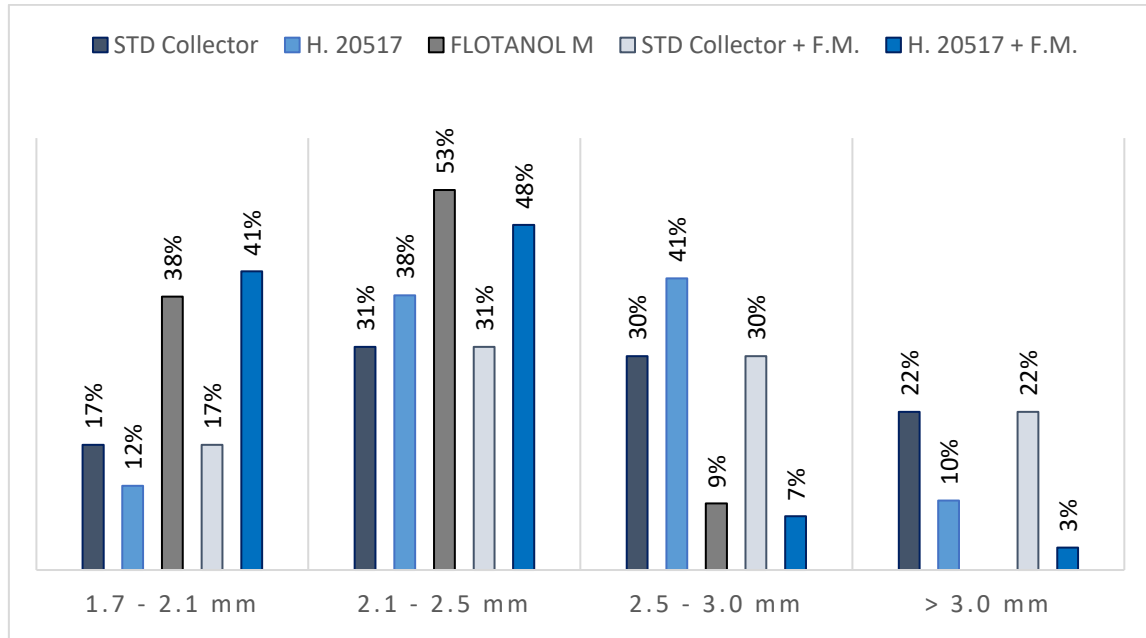


Figure 7. The synergistic effect of the new collectors with the standard frother FLOTANOL M.

### 3.1.5 Flotation results: Physico-chemical strategy to increase the performance of collectors for CPF

Figure 8 illustrates the differences in performance comparing the new collector HOSTAFLOT 20517 with the standard collector, plus a comparison with the traditional sulphide flotation collectors - SIPX, SIBX and PAX. The overall rougher recovery obtained with the H. 20517 is 80.9%, 11.7 pp compared to SIBX and 2.2 pp higher than the standard collector, yielding the same mass pull.

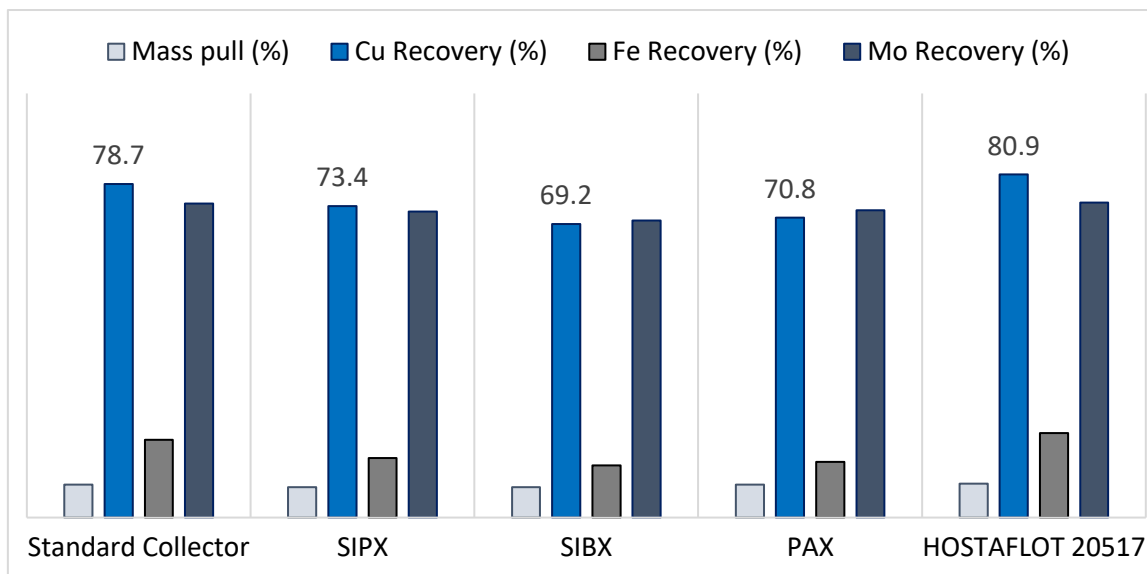


Figure 8. Flotation performance comparing different copper sulphide collectors in pH 8.5

Figure 9 shows that the standard collector yields a copper recovery of 33% out of the coarse particles (+210  $\mu\text{m}$  fraction), whereas the new collector HOSTAFLOT 20517 yields a copper recovery of 43%, meaning a 10 percentage points increase in the coarse fraction. Moreover, an additional copper recovery of 6 percentage points was obtained for the +150  $\mu\text{m}$ , totalizing an increase of 16 percentage points only by replacing the standard collector by the HOSTAFLOT 20517.

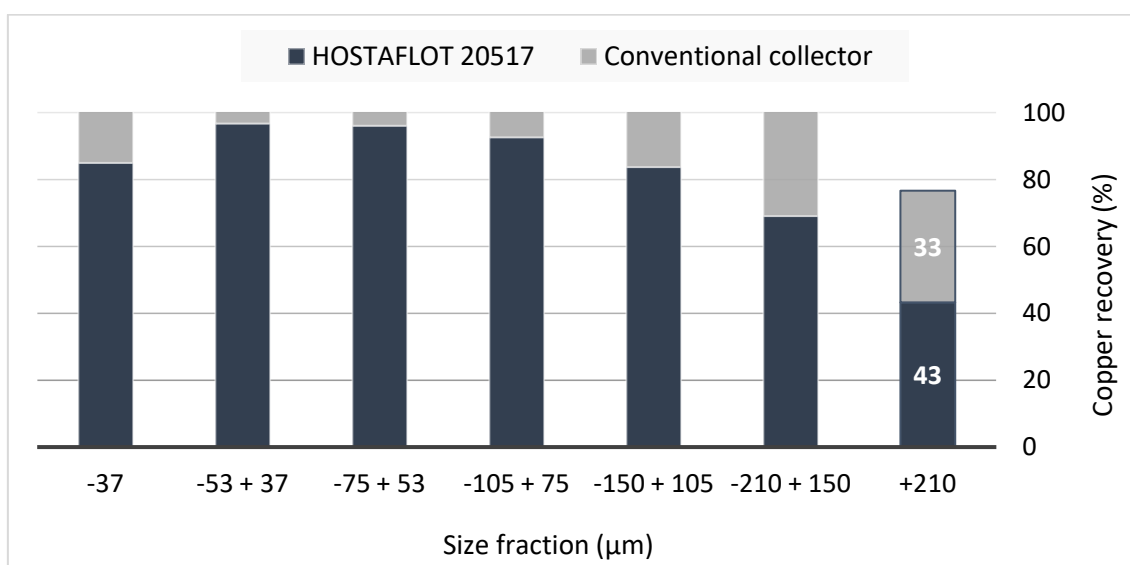


Figure 9. Assay by size comparing copper recovery obtained with standard collector against the new collector HOSTAFLOT 20517

By correlating the fundamental studies and the flotation performance, the following effects of the specialty collector on the floatability of coarse and unliberated chalcopyrite particles were identified:

- Lower Redox potential compared to the standard collector, which indicates stronger adsorption.
- Contact angle significantly higher compared to the standard collector, relevant to increase the recovery of the +210  $\mu\text{m}$  particles.
- When combined to the FLOTANOL M frother, bubble size distribution was narrowed down by the use of HOSTAFLOT 20517, keeping bubbles concentrated in the 1.7 mm to 2.5 mm range, whereas the standard collector caused a broad BSD, with 22% of the bubbles surpassing 3.0 mm.
- The recovery of Copper increase in 16% considering the fraction +150  $\mu\text{m}$ , replacing the standard collector by the HOSTAFLOT 20517.

### **3.2 The effect of specialty frother on the Coarse Particle Flotation hydrodynamics**

Aiming at elucidating the mechanisms behind the higher performance of the FLOTANOL C07 over the frother FLOTANOL M, which is a MIBC based frother, bubble size distribution and rheology analysis were conducted and discussed by the light of the flotation results recently published by Carvalho et al. (2025) and Killström (2024).

According to the authors, FLOTANOL C07 is a stronger frother compared to alcohol and conventional PPG frothers. Therefore, when tested in the hydrofloat the frother associated with optimized hydrodynamic conditions yielded up to 81.9% copper recovery in the +150  $\mu\text{m}$  fraction, a very high recovery compared to the 94.8% recovery in the -150  $\mu\text{m}$  fraction (CARVALHO et al., 2025).

Killström (2024) showed FLOTANOL C07 yielded the best recovery out of every other frother tested for a coarse particle copper ore. The +450  $\mu\text{m}$  copper recovery was 94% and for particles under 106  $\mu\text{m}$ , 90,5%, which are both very good recoveries (KILLSTRÖM, 2024).

Therefore, the following sections discuss the differences between the FLOTANOL M (MIBC based frother) and FLOTANOL C07 (glycol based frother), specifically over the CPF cell hydrodynamics.

### 3.2.1 Bubble Size and Surface Tension

Table 1 exhibits the differences in the CCC, the bubble Sauter diameter ( $D_{3,2}$ ) and surface tension (SFT) for the two studied frothers: FLOTANOL M (alcohol type frother) and FLOTANOL C07 (glycol type frother).

The frother FLOTANOL C07 showed a CCC much smaller compared to the FLOTANOL M (Figure 10), which is caused by the sharp negative slope on the SFT reduction from 72.8 mN/m to 65.8 mN/m with 10 mg/L of the FLOTANOL C07 (Figure 11). Diversely, the FLOTANOL M did not cause significant changes in the SFT in this dosage.

Accordingly, the weighted mean bubble size is 1.7 mm for the alcohol frother against 1.0 mm for the glycol-based chemistry. Additionally, Figure 12 shows the frother FLOTANOL C07 yields a narrow BSD, concentrated in the fine fraction (from 0.7 mm to 1 mm), while the FLOTANOL M generates a broad distribution of bubbles in the coarse range.

Table 1 – Comparison of frother parameters: FLOTANOL M versus FLOTANOL C07

Frother	CCC (mg/L)	$D_{3,2}$ (mm) 10 mg/L	SFT (mN/m) 10 mg/L
FLOTANOL M	13	1.7	72.3
FLOTANOL C07	4	1.0	65.8

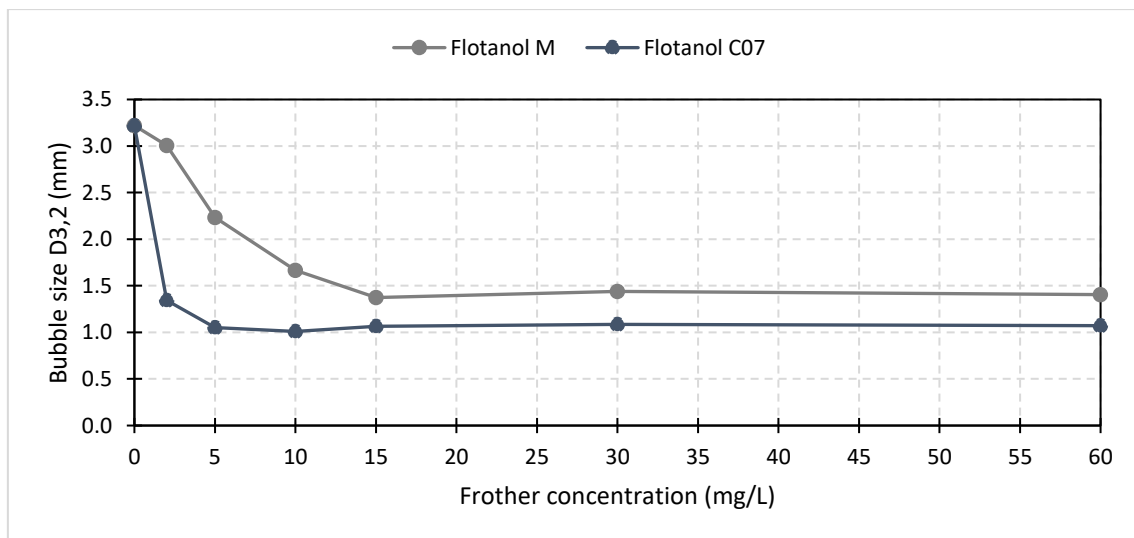


Figure 10. Bubble Sauter Diameter ( $D_{3,2}$ ) as a function of different dosages of the studied frothers



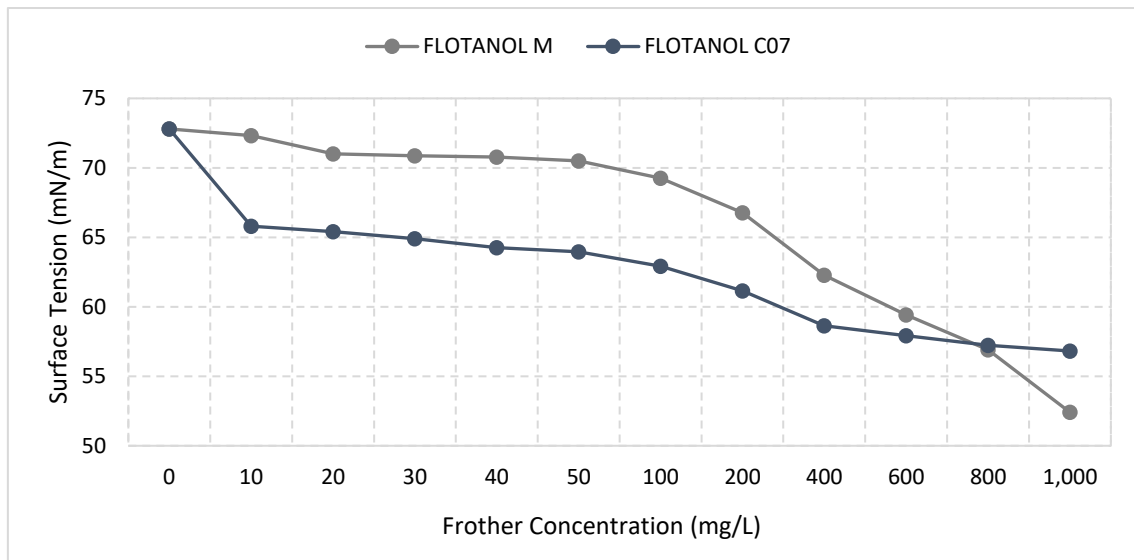


Figure 11. Surface tension as a function of different concentrations of the studied frothers

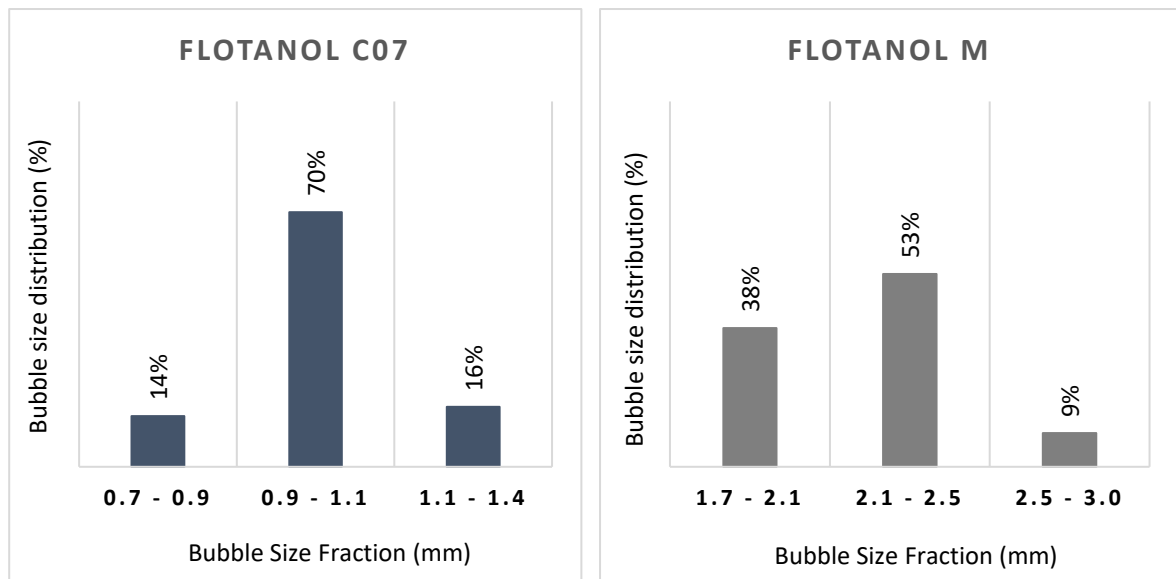


Figure 12. Bubble size distribution charts comparing the percentage of bubbles in three different size ranges for the studied frothers.

In fluidized-bed flotation systems such as the HydroFloat®, the control of bubble size distribution is central to maximizing coarse particle recovery. A narrower distribution of finer bubbles, as provided by the FLOTANOL C07 (Figure 12a), creates a more uniform hydrodynamic environment, where bubbles of similar size rise at comparable velocities, reducing segregation and minimizing turbulent shear. This homogeneity enhances the probability of bubble–particle collisions while ensuring that attached coarse particles experience consistent lift forces, lowering the risk of detachment. In addition, finer

bubbles provide a larger total surface area at a given gas rate, thereby increasing collision frequency and stabilizing bubble–particle aggregates across the bed (ANZOOM; BOURNIVAL; ATA, 2024).

By contrast, a broad distribution with a significant fraction of coarse bubbles, as yielded by the FLOTANOL M (Figure 12b), generates uneven flow fields and large voids in the pulp, which reduces the effective surface area for attachment and introduces higher local turbulence around rising macro-bubbles. Such conditions are detrimental to coarse, weakly hydrophobic particles, as they favor premature detachment and reduce overall carrying capacity (SHAHBAZI; REZAEI, 2008).

Therefore, the use of frothers that promote a narrow distribution of finer bubbles aligns with the CPF equipment design principle of combining low-turbulence fluidization with enhanced bubble–particle stability, enabling more efficient recovery of coarse and unliberated chalcopyrite.

### 3.2.2 Bubble Size and pulp rheology: The role of the frother in bubble-particle stability through the fluidized bed

Table 2 conveys the rheological parameters extracted from the Hershel-Bulkley model for the FLOTANOL M and for the FLOTANOL C07. These parameters were utilized to calculate the apparent viscosity caused by the frothers in the fluidized bed with shear rates ranging from 10 to 100 s<sup>-1</sup>, the typical turbulence rate caused by the bubble-particle-fluid flow in the separation zone and the maximum micro shear rate resultant in the bubble-coarse particle interface.

Table 2. Herschel-Bulkley parameters determined for the evaluated frothers

<b>Frother</b>	<b>Dosage (g/t)</b>	<b><math>\tau_0</math></b>	<b>K</b>	<b>n</b>	<b>r</b>
Flotanol M	12	0.082	0.019	1.631	0.998
Flotanol C07	12	0.096	0.002	2.154	0.996

Table 3. Viscosity calculations based on the Herschel-Bulkley parameters determined for the evaluated frothers

Shear rate ( $s^{-1}$ )	$\eta$ (n=1.6, F.M.)	$\eta$ (n=2.2, F.C07)	Ratio $\eta_2/\eta_1$	% increase
10	1.000	2.512	2.512	151%
30	3.660	18.384	5.024	402%
50	7.069	54.737	7.743	674%
100	15.849	251.189	15.849	1448%

The chemical tuning of rheology ensures the fluidized bed maintains a low-shear, hindered-settling environment where detachment forces are minimized and coarse particle recovery is maximized. Fluidized-bed flotation cells, where an upward flow of water creates a hindered settling environment. The frother FLOTANOL C07 improves the fluidized bed hydrodynamics in ways beyond bubble generation:

- Drag reduction and energy dissipation: FLOTANOL C07 reduced bubble coalescence, maintaining a high surface area of stable bubbles, which also modified the apparent viscosity and turbulence spectrum of the fluidized bed, as seen in Table 3. This is because more homogeneous gas dispersion lowers localized shear stresses, that could cause the detachment of coarse particle–bubble aggregates.
- Microhydrodynamics at particle scale: FLOTANOL C07 produces more stable bubbles, due to the coating with viscoelastic frother films, that generate lubrication layers when interacting with coarse particles. This lowers the energy barrier for attachment and cushions aggregates against detachment during fluidization.
- Bed permeability and selective transport: FLOTANOL C07 can indirectly increase the rheological yield stress of the fluidized suspension by altering the stability of the film between gas and solids. A stable bubble network prevents particle settling without creating overly viscous hydrodynamic line flows. This is key to balancing selective recovery (hydrophobic coarse particles attach and rise) against gangue rejection (hydrophilic coarse particles remain in the fluidized bed and are rejected).

#### **4. Conclusion**

The flotation and fundamentals studies demonstrate that the specialty collector for CPF (HOSTAFLOT 20517) provides clear advantages over conventional reagents for the flotation of coarse and unliberated chalcopyrite. By lowering redox potential and increasing contact angle, the collector enhanced surface hydrophobicity and improved the recovery of particles above 210  $\mu\text{m}$ . In synergy with the frother FLOTANOL M, HOSTAFLOT 20517 also produced a narrower and more favorable bubble size distribution, avoiding the formation of excessively large bubbles. These effects translated into a 16% increase in copper recovery in the +150  $\mu\text{m}$  fraction, highlighting the potential of tailored collector–frother systems to extend the flotation limits of coarse particles. Additionally, bubble size and rheology analysis confirmed that specialty frothers for CPF not only stabilize bubbles but also fine-tune the hydrodynamics and microhydrodynamics of the fluidized bed and bubble-particle interface. By modifying dispersion, energy dissipation, and particle–bubble microinteractions, specific frothers such as the FLOTANOL C07 create a suspension environment that supports enhanced recovery of coarse particles that would otherwise detach and settle in CPF systems.

## References

- Anzoom, S. J.; Bournival, G.; ATA, S. (2024). *Coarse particle flotation: A review*. Minerals Engineering. Volume 206, 2024, 108499, ISSN 0892-6875.
- Carvalho, M., et al. (2025). *Enhanced coarse particle flotation: A novel CPF cell* (pilot trial / journal article). International Journal of Mineral Processing / Procedia (2025).
- Castellón, C.I.; Toro, N.; Gálvez, E.; Robles, P.; Leiva, W.H.; Jeldres, R.I. Froth Flotation of Chalcopyrite/Pyrite Ore: A Critical Review. *Materials* **2022**, *15*, 6536. <https://doi.org/10.3390/ma15196536>
- Islam, M. T., & Nguyen, A. N. (2019). *A numerical study with experimental validation of liquid-assisted fluidization of particle suspensions in a HydroFloat cell*. Minerals Engineering, 134, 176–192.
- Killström, N. (2024). *Evaluation of frother strength for coarse particle flotation* (Master's thesis). University of Oulu. <https://urn.fi/URN:NBN:fi:oulu-202408165473>
- Kohmuench, J. N., et al. (2018). *Improving coarse particle flotation using the HydroFloat™* (conference/journal paper). Minerals Engineering / conference proceedings.
- Li, D., & Yuan, Z. (2022). *Bubble behaviour investigation in a wet fluidized bed using digital image analysis*. Canadian Journal of Chemical Engineering.
- Miki, Hajime; Matsuoka, Hidekazu; Hirajima, Tsuyoshi; Suyantara, Gde Pandhe Wisnu; Sasaki, Keiko. "Electrolysis Oxidation of Chalcopyrite and Molybdenite for Selective Flotation." *Materials Transactions*, Vol. 58, No. 5 (2017), pp. 761–767. DOI: 10.2320/matertrans.M-M2017807
- Opoku, P. A., et al. (2025). *An overview of coarse particle beneficiation of lithium ores*. Scientific Reports / Nature.
- Regino, N., et al. (2020). *A comparison of two circuit applications for implementation of HydroFloat®* (Eriez technical report / conference paper). Eriez / Minerals Engineering conference paper.
- Shahbazi, B., & Rezaei, B. (2008). "Bubble-Particle Attachment Probability on Coarse Particles Flotation." *Asian Journal of Chemistry*, 20(3), 2238–2250.
- Wang, L., Peng, Y., & others. (2020). *A Brief Review of Pulp and Froth Rheology in Mineral Flotation*. Journal of Chemistry.
- Xing, Y., Xu, M., Gui, X., Cao, Y., Babel, B., Rudolph, M., Weber, S., Kappl, M., & Butt, H.-J. (2024). *Effect of Particle Size and Hydrophobicity on Bubble-Particle Collision Detachment at the Slurry-Foam Phase Interface*. ACS Omega.
- Zheng, et al. (2012). *Quantifying rheological and fine particle attachment contributions to coarse particle recovery in flotation*. Minerals Engineering, 39, 89-97.
- Yang, X.; Li, Y.; Chen, W.; Duan, W.; Xiao, Q.; Jiang, T. A Quantitative Relationship between Oxidation Index and Chalcopyrite Flotation Recovery. *Minerals* **2022**, *12*, 888. <https://doi.org/10.3390/min12070888>
- Yelloji Rao, M.K., Natarajan, K.A. Effect of electrochemical interactions among sulfide minerals and grinding medium on chalcopyrite flotation. *Mining, Metallurgy & Exploration* **6**, 146–151 (1989). <https://doi.org/10.1007/BF03402706>